Food Chemistry 237 (2017) 1163–1171

Contents lists available at ScienceDirect

Food Chemistry

journal homepage: www.elsevier.com/locate/foodchem

Structural characterization, formation mechanism and stability of curcumin in zein-lecithin composite nanoparticles fabricated by antisolvent co-precipitation

Lei Dai, Cuixia Sun, Ruirui Li, Like Mao, Fuguo Liu, Yanxiang Gao *

Beijing Advanced Innovation Center for Food Nutrition and Human Health, Beijing Laboratory for Food Quality and Safety, Beijing Key Laboratory of Functional Food from Plant Resources, College of Food Science & Nutritional Engineering, China Agricultural University, Beijing 100083, PR China

ARTICLE INFO

Article history:
Received 8 January 2017
Received in revised form 22 May 2017
Accepted 26 May 2017
Available online 1 June 2017

Keywords:
Zein-lecithin composite nanoparticles
Curcumin
Antisolvent co-precipitation
Delivery
Mechanism

ABSTRACT

Curcumin (Cur) exhibits a range of bioactive properties, but its application is restrained due to its poor water solubility and sensitivity to environmental stresses. In this study, zein-lecithin composite nanoparticles were fabricated by antisolvent co-precipitation technique for delivery of Cur. The result showed that the encapsulation efficiency of Cur was significantly enhanced from 42.03% in zein nanoparticles to 99.83% in zein-lecithin composite nanoparticles. The Cur entrapped in the nanoparticles was in an amorphous state confirmed by differential scanning calorimetry and X-ray diffraction. Fourier transform infrared analysis revealed that hydrogen bonding, electrostatic interaction and hydrophobic attraction were the main interactions among zein, lecithin, and Cur. Compared with single zein and lecithin nanoparticles, zein-lecithin composite nanoparticles significantly improved the stability of Cur against thermal treatment, UV irradiation and high ionic strength. Therefore, zein-lecithin composite nanoparticles could be a potential delivery system for water-insoluble bioactive compounds with enhanced encapsulation efficiency and chemical stability.

1. Introduction

Many bioactive compounds (e.g., carotenoids, polyphenols and conjugated lipids) are beneficial to maintain human health and prevent certain chronic diseases even with relatively low level. As a natural polyphenolic compound, curcumin (Cur) [1, 7-bis (4-hydroxy-3-methoxyphenyl)-1, 6-hepadiene-3, 5-dione], a natural polyphenolic compound, can be obtained from the rhizome of turmeric (*Curcuma longa*), and is commonly used as a seasoning ingredient or colorant in foods (Xiao, Nian, & Huang, 2015). Recent studies have shown that Cur exhibits a range of biological activities including antioxidant and anti-tumor activities, and it is also helpful in inhibiting neurodegenerative diseases (Aditya et al., 2013; Shahgholian & Rajabzadeh, 2016; Wilken, Veena, Wang, & Srivatsan, 2011). Moreover, Cur has a low toxicity and very good safety profile even at a relatively high doses (as high as 8 g/day) (Anand, Kunnumakkara, Newman, & Aggarwal, 2007; Cheng et al., 2001). However, the application of Cur is limited due to its poor water solubility, sensitivity to environmental stresses and low oral bioavailability (Jafari, Sabahi, & Rahaie, 2016). Therefore, it is required to explore suitable approaches to overcome the aforementioned problems and broaden the application of Cur. Cur in food-grade colloidal delivery systems has been regarded as an appropriate choice to overcome the limitation of Cur in commercial products. Various types of colloidal delivery systems such as polysaccharide-based hydrogel beads (Zhang et al., 2016), nanoemulsions (Li, Hwang, Chen, & Park, 2016), nanoparticles (Hu et al., 2015), liposomes (Chen et al., 2015) have been utilized to encapsulate and protect Cur. Among these systems, the nanoparticles formed by food-grade proteins have presented a good performance in enhancing the functional properties for Cur (Sadeghi et al., 2014).

Zein, a major storage protein in corn, consists of four major components: α, β, γ, and δ-zein, and more than 50% of amino acid residues in zein are hydrophobic, which make it soluble in aqueous ethanol solution (60–90%), but insoluble in water (Hu & McClements, 2015). Due to its highly hydrophobic nature, zein can be easily converted into spherical colloidal nanoparticles by the antisolvent precipitation method (ASP), which make it particularly suitable to deliver functional components, which have a low solubility in water but are soluble in ethanol (Chen, Zheng, McClements, & Xiao, 2014). In the past decades, zein has been widely utilized to fabricate nanoparticles for the encapsulation of

* Corresponding author at: Box 112, No. 17 Qinghua East Road, Haidian District, Beijing 100083, PR China.
E-mail address: gyxcau@126.com (Y. Gao).

http://dx.doi.org/10.1016/j.foodchem.2017.05.134
0308-8146/

functional components such as lutein (Hu, Lin, Liu, Li, & Zhao, 2012), quercetagetin (Q; Sun et al., 2015), Cur (Patel, Hu, Tiwari, & Velikov, 2010), and α-tocopherol (Luo, Zhang, Whent, Yu, & Wang, 2011). Nevertheless, zein nanoparticles usually have low encapsulation efficiency (EE). To improve the physical stability and functional properties of zein-based nanoparticles, the ASP was used to produce zein- biopolymer composite colloidal particles with a core-shell structure, which consisted of a zein core and a biopolymer shell. The commonly applied biopolymers were pectin (Hu et al., 2015), sodium caseinate (Chen & Zhong, 2014; Patel, Bouwens, & Velikov, 2010), chitosan (Luo et al., 2011), and sodium alginate (Zou et al., 2016). Furthermore, some small molecular surfactants have also been applied as shells to prevent the aggregation of zein nanoparticles by reducing the surface hydrophobicity, increasing electrostatic and steric repulsion. Gao et al. (2014) showed that zein and sodium stearate complex was generated through the nonspecific hydrophobic attraction and improved the solubility, diffusive mobility and interfacial loading of zein. Hu and McClements (2014) used a food-grade nonionic surfactant (Tween 80) as a stabilizer to form a core–shell structure with zein. A similar study also reported that the combination of lecithin and Pluronic F68 was able to improve the stability of zein nanoparticles (Podaralla & Perumal, 2012). Nevertheless, the method of anti-solvent co-precipitation (ASCP) were also used to prepare zein based complexes. In our published article, Q-loaded zein- propylene glycol alginate (PGA) binary complexes were fabricated by using ASCP technique due to the good solubility of zein, PGA and Q in aqueous ethanol solution. The result showed that a synergistic effect was found between zein and PGA on improving the EE and loading capacity of Q (Sun, Dai, & Gao, 2016).

Lecithin is considered as a safe and biocompatible excipient and has already been widely applied in food, pharmaceutical, and cosmetic industries. It consists of a glycerol backbone esterified with fatty acids and a phosphate group, and has a good emulsifying property and is widely used in food-grade emulsions (Xue & Zhong, 2014). Recent investigations reported that lecithin based colloidal delivery systems could be suitable carriers for bioactive ingredients. Souza et al. (2014) reported that quercetin loaded in lecithin and chitosan nanoparticles had a higher encapsulation efficiency up to 96.13%, and improved antioxidant activity when compared to free quercetin. Xue and Zhong (2014) also presented that the gelatin and lecithin complex had the synergistic surface activity and could form stable thymol nanodispersions. Our previous study confirmed that lecithin could interact with zein in aqueous ethanol solution and form stable composite colloidal nanoparticles (Dai, Sun, Wang, & Gao, 2016). Zein-lecithin composite nanoparticles as a carrier for the delivery of bioactive components might have a promising potential.

In this study, the ASCP approach was used to fabricate Cur-loaded zein-lecithin composite nanoparticles. The composite nanoparticles were characterized in terms of particle size, turbidity and zeta potential. Florescence spectroscopy, Fourier transform infrared spectroscopy (FTIR), X-ray diffraction (XRD) and differential scanning calorimetry (DSC) were used to identify the driving forces for the formation of composite nanoparticles and the physical state of encapsulated Cur. Furthermore, the morphological structure, photochemical and thermal stability were also investigated. Findings from this study might provide a new idea of developing new carriers for the delivery of bioactive compounds.

2. Material and methods

2.1. Materials

Zein with a protein content of 91.3% (w/w) was purchased from Sigma-Aldrich (St. Louis, MO, USA). Soy lecithin (S-100, 94% phosphatidylcholine) was from Lipoid (Ludwigshafen, Germany). Cur (98% purity) was purchased from China National Medicine Group Shanghai Corporation (Shanghai, China). Absolute ethanol (99.99%), solid sodium hydroxide, liquid hydrochloric acid (36%, w/w) and sodium chloride were acquired from Eshowbokoo Biological Technology Co., Ltd. (Beijing, China).

2.2. Preparation of Curcumin-loaded zein-lecithin composite nanoparticles

Briefly, 1.0 g zein was dissolved in 100 mL 70% (v/v) aqueous ethanol solution with magnetic stirring at 600 rpm for 2 h. Then different amounts of soy lecithin were added to the zein aqueous ethanol solution to reach zein to lecithin mass ratios of 10:1, 5:1, 2:1, 1:1, 2:3 and 1:2, respectively, under continuous stirring (600 rpm) for 3 h. The mixed solutions were allowed to stand for 2 h at room temperature (25 °C). The Cur (zein to Cur mass ratio of 10:1) was added to the zein-lecithin solution and stirred (600 rpm) for 1 h. Approximately 20 mL zein-lecithin-Cur aqueous ethanol solution was slowly injected (using a syringe) into 60 mL deionized water with a constant stirring at 600 rpm for 30 min to form dispersions. The ethanol remained in dispersions was evaporated by a rotary evaporator at 45 °C. And the dispersions were adjusted to pH 4.0 using 0.1 N HCl or NaOH. The Cur-loaded zein, Cur-loaded lecithin and zein-lecithin colloidal dispersions were obtained by the aforementioned process and used as the controllers. The composite nanoparticle dispersions were subjected to centrifugation at 725*g* (Sigma 3k15, Germany) for 20 min to separate large particles and free Cur if any. Finally, the dispersions were stored in the refrigerator at 4 °C for further analysis, and parts of the dispersions were freeze-dried for 48 h with an Alpha 1–2 D Plus freeze-drying apparatus (Marin Christ, Germany) to acquire dry particles. Samples with zein to lecithin mass ratios of 100:0, 10:1, 5:1, 2:1, 1:1, 2:3, 1:2 and 0:100 were named as Cur/Z, Cur/Z-$L_{10:1}$, Cur/Z-$L_{5:1}$, Cur/Z-$L_{2:1}$, Cur/Z-$L_{1:1}$, Cur/Z-$L_{2:3}$, Cur/Z-$L_{1:2}$, Cur/L respectively.

2.3. Particle size, zeta (ζ)-potential and turbidity measurements

Particle size and ζ-potential of colloidal dispersions were determined by using a combined dynamic light scattering (DLS) and particle electrophoresis instrument (Zetasizer Nano-ZS90, Malvern Instruments Ltd., Worcestershire, UK) according to the descriptions in our previous report (Sun et al., 2016). The particle size reported as cumulative mean diameter (size, nm) was calculated based on the intensity weighted diameter using the Stokes-Einstein equation. The ζ-potential of the particles was obtained by using the Smoluchowski model through an electrophoretic mobility measurement performed in a capillary electrophoresis device inserted into the DLS instrument. All measurements were carried out at 25 °C.

Nephelometry experiments were performed in a HACH 2100N laboratory turbidimeter (Loveland, Colorado, USA) following the method described by Sun et al. (2015). The optical apparatus was equipped with a tungsten-filament lamp with three detectors: a 90° scattered-light detector, a forward-scatter light detector and a transmitted light detector. The calibration was performed using a Gelex Secondary Turbidity Standard Kit (HACH, Loveland, USA).

2.4. Encapsulation and loading efficiency

The EE and LE of Cur were determined according to the method of Gomez-Estaca, Balaguer, Gavara, and Hernandez-Munoz (2012) with some modifications. The Cur/Z, Cur/L and Cur/Z-L nanoparticle dispersions were diluted by absolute ethanol to reach an ethanol concentration of 80% (v/v) with the aid of ultrasonication. The

Cur content was determined using a UV-1800 spectrophotometer (Shimadzu Corporation, Kyoto, Japan). Absorbance at the wavelength of 426 nm was recorded. EE and LE were calculated by following the equations below:

$$EE(\%) = \frac{encapsulated\ curcumin\ (mg)}{total\ curcumin\ input\ (mg)} \times 100$$

$$\mathrm{LE}(\%) = \frac{encapsulated\ curcumin\ (mg)}{weight\ of\ zein\ and\ lecithin\ (mg)} \times 100$$

2.5. Photostability

In order to evaluate the effect of carriers on the stability of Cur in the nanoparticles against UV photolysis, stability of free Cur and the encapsulated Cur in zein-lecithin composite nanoparticles were tested following the method reported by Xiao et al. (2015). Briefly, 5 mL of freshly prepared Cur, Cur/Z, Cur/L and Cur/Z-L dispersions were placed into transparent glass vials. Then samples were put in a controlled light cabinet (Q-Sun, Q-Lab Corporation, Ohio, USA) for up to 2 h. The sampling was carried out at designed time intervals of 30, 60, and 90 min. The quantity of Cur remained was determined through spectrophotometry analysis as described in the aforementioned section. The retention rate of Cur was plotted against treatment time.

2.6. Thermal stability

Briefly, 5 mL of freshly prepared Cur, Cur/Z, Cur/L and Cur/Z-L nanoparticle dispersions were placed into transparent glass vials and incubated in water bath at different temperatures (75, 85 and 95 °C) for 30 min and cooled down to room temperature (25 °C). The quantity of Cur remained in samples was then determined spectrophotometrically.

2.7. Fluorescence spectroscopy

Fluorescence measurements were carried out using a fluorescence spectrophotometer (F-7000, Hitachi, Japan) following the method described by Xiao et al. (2015) with some modifications. Fluorescence spectra of pure Cur (1 mg Cur dissolved in 1 mL 70% aqueous ethanol solution and then mixed with 3 mL deionized water), Cur/Z and Cur/Z-L nanoparticle dispersions were recorded. The emission spectra were collected from 450 to 700 nm with an excitation wavelength of 420 nm using a quartz cell with a 10 mm path length. The excitation and emission bandwidths were set at 5 nm. All data were collected at room temperature (25 °C).

2.8. XRD

The molecular arrangements of zein, Cur, lecithin, as well as the Cur/Z, zein-lecithin and Cur/Z-L nanoparticles in powder, were determined by XRD patterns at room temperature (25 °C). XRD patterns were recorded using a Bruker D8 X-ray diffractometer (Brucker D8, Odelzhausen, Germany) based on the method of Patel, Hu et al. (2010) and Patel, Bouwens et al. (2010). The instrument was equipped with a copper anode, and working with an accelerating voltage of 40 kV and a tube current of 40 mA. The data was collected over an angular range from 5° to 55° in continuous mode using a step size of 0.02° and step time of 5 s.

2.9. FTIR

The chemical structures of pure ingredients (zein, Cur, lecithin) and nanoparticles (Cur/Z, zein-lecithin, and Cur/Z-L) were investigated by a Spectrum 100 Fourier transform spectrophotometer (Perkin-Elmer, Warrington, UK). Briefly, 2.0 mg sample was mixed with 198 mg pure potassium bromide (KBr) powder. Then the mixture was ground into fine powder, pressed into pellet and measured by FTIR. The spectra were collected at the wavenumbers of 400–4000 cm^{-1} in 64 scans with a resolution of 4 cm^{-1}. The spectrum of pure KBr powder was used as a baseline. The data was analyzed using the software OMNIC 8.2 (Thermo Fisher Scientific Inc., Waltham, MA, USA).

2.10. DSC

The thermal characteristics of pure Cur and nanoparticles (Cur/Z and Cur/Z-L at different mass ratios of zein to lecithin) were studied using a differential scanning calorimeter (DSC-60, Shimadzu, Tokyo, Japan). About 5 mg freeze-dried sample was weighted in a standard aluminum pan and hermetically sealed. The lids were pinned with a syringe needle to exclude the interference of moisture. An empty sealed aluminum pan was applied as a reference. Samples were heated from 30 to 200 °C at 10 °C/min with a constant purging of dry nitrogen at a rate of 20 mL/min. For comparison, DSC thermograms of physical mixtures of zein, lecithin and Cur were also collected.

2.11. Effect of salt on the stability of nanoparticle dispersions

The effect of salt on the stability of Cur/Z and Cur/Z-L nanoparticles was evaluated according to the method of Chen et al. (2014) with some modifications. The colloidal dispersions were diluted with the same volume of sodium chloride solution to reach different salt concentrations (0–300 mM NaCl). The samples were stored at 4 °C overnight for stability analysis.

2.12. AFM

The morphology of colloidal nanoparticles was observed by AFM (DI Nanoscope TV, Veeco Company, Plainview, NY) equipped with an E-scanner. Tapping mode with nominal spring constant of 20–100 N m^{-1} and nominal resonance frequencies of 10–200 kHz were employed. The diluted samples were immediately spread evenly onto freshly cleaved mica sheets mounted on sample disks with great care and air-dried for more than 3 h before AFM scans were taken.

2.13. Scanning electron microscopy and energy dispersive spectrometer (SEM-EDS)

The micro-morphology of nanoparticles was observed by SEM (Hitachi S-480). The elemental compositions of the samples were obtained by an X-ray microanalysis system (HORIBA EX-350) which was coupled with SEM. Tiny amount of dried powders was mounted on aluminum stubs with double-sided adhesive and coated with a gold layer to avoid charging under the electron beam.

2.14. Statistical analysis

All the data obtained were average values of triplicate determinations and subjected to statistical analysis of variance using SPSS 18.0 for Windows (SPSS Inc., Chicago, USA). Statistical differences were determined by one-way analysis of variance (ANOVA) with Duncan's post hoc test and differences were considered to be significant with $P < 0.05$.

3. Results and discussion

3.1. Particle size, ζ-potential and turbidity

The effects of lecithin level on the particle size, ζ-potential and turbidity of the composite nanoparticles were summarized in Table 1. The mean size of the Cur/Z and Cur/L nanoparticles was 178 and 237 nm, respectively. The size of Cur/Z-L composite nanoparticles varied with the mass ratio of zein to lecithin. As the level of lecithin was increased, the size of Cur/Z-L composite nanoparticles was firstly increased and then decreased. At the zein to lecithin mass ratios of 10:1 and 5:1, the sizes of Cur/Z-L composite nanoparticles were higher (228 and 428 nm) than these of the Cur/Z nanoparticles (178 nm). Gao et al. (2014) reported that the C16 alkyl chain of sodium stearate (SS) was probably incorporated into the hydrophobic region of zein structure, forming the zein−SS complexes with partially unfolded hydrophobic microdomains and increasing the anisotropy accompanying partial unfolding of zein, which could contribute to the large particle size. However, further increase in lecithin concentration led to markedly ($P < 0.05$) decrease of particle size from 428 to 288, 141, 124, and 131 nm for samples of Cur/Z-$L_{2:1}$, Cur/Z-$L_{1:1}$, Cur/Z-$L_{2:3}$ and Cur/Z-$L_{1:2}$ composite nanoparticles, respectively. This result might be due to zein and lecithin could form a compact structure at relatively high level of lecithin, decreasing the size of composite nanoparticles.

Nephelometry was used to study the physical–chemical driving forces involved in the formation of zein, lecithin and Cur composite nanoparticles. Turbidity can be influenced by some factors such as the particle size, refractive index, ζ-potential and color of the sample as well as particle interactions including micro- and nano-aggregation (Wang, Liu, & Gao, 2016). As shown in Table 1, the changing trend of turbidity was consistent with that of particle size. The turbidity of the Cur/Z nanoparticle dispersions was 464 NTU. With the increase of lecithin level, the turbidity of Cur/Z-L composite nanoparticle dispersions was enhanced. This result might be ascribed to the large size of Cur/Z-L composite nanoparticles, especially for the sample of Cur/Z-$L_{5:1}$, whose particle size was 428 nm. Wang et al. (2016) pointed out that the increase in turbidity was ascribed mostly to the micro-aggregation of the complexes. Further increase in the level of lecithin, the turbidity of Cur/Z-L composite nanoparticle dispersions was greatly ($P < 0.05$) decreased from 974 to 681, 389, 255 and 293 NTU, for the samples of Cur/Z-$L_{2:1}$, Cur/Z-$L_{1:1}$, Cur/Z-$L_{2:3}$ and Cur/Z-$L_{1:2}$, respectively.

In the absence of lecithin, the ζ-potential of Cur/Z nanoparticles was + 26 mV. After the addition of lecithin, the ζ-potential values were significantly ($P < 0.05$) decreased from +26 to +23,+16, +7 and +5 mV, for Cur/Z-L composite nanoparticles at the mass ratios of 10:1, 5:1, 2:1 and 1:1, respectively. The ζ-potential values of Cur/Z-$L_{2:3}$ and Cur/Z-$L_{1:2}$ were slightly changed with the increase of lecithin concentration. Patel, Hu et al. (2010); Patel, Bouwens et al. (2010) reported that zein and Cur nanoparticles prepared by precipitation process in water had positively charged surface and the ζ-potential of the nanoparticles was gradually decreased with the increase of Cur concentration. The ζ-potential of Cur/L nanoparticles was −2.19 mV. These results were consistent with the report of Sebaaly, Jraij, Fessi, Charcosset, and Greige-Gerges (2015). The increased concentration of the hydrophobic lecithin in the particle interior and probably on the particle surface reduced the ζ-potential of composite nanoparticles. Hu and McClements (2014) also interpreted that the positive charge of the zein nanoparticles was decreased in the presence of Tween 80, attributing to the adsorption of a layer of non-ionic surfactant on the surface of nanoparticles.

3.2. Encapsulation and loading efficiency

The EE and LE of Cur/Z, Cur/L and Cur/Z-L nanoparticles were also shown in Table 1. In the absence of lecithin, the EE of Cur loaded in zein nanoparticles was around 42.03%. There was a gradual increase in the EE of Cur in zein-lecithin composite nanoparticles with the rise of lecithin concentration. The EE of Cur/Z-L composite nanoparticles was significantly ($P < 0.05$) increased from 42.03 to 99.83% at the zein to lecithin mass ratio of 1:2, compared to that of Cur/Z. The EE of Cur/L was 86.78%, which was lower than that of Cur/Z-L composite nanoparticles at the mass ratios of 5:1, 2:1, 1:1 and 1:2, respectively. As the level of lecithin was increased, the average LE of Cur in zein-lecithin composite nanoparticles (Cur/Z-$L_{5:1}$ and Cur/Z-$L_{2:1}$) was significantly ($P < 0.05$) enhanced. This result confirmed that there was a synergistic effect between zein and lecithin on improving the EE and LE of Cur. The lecithin might promote to entrap the Cur adherent on the surface of zein or free Cur in the composite nanoparticles. Moreover, lecithin could form a complex with free Cur, which increased encapsulation and loading efficiency.

3.3. Photo and thermal stability

The application of Cur was limited by its sensitivity to various environmental stresses, e.g., light, heat, oxygen. In the present study, the stability of the entrapped Cur under ultraviolet light and thermal treatment was explored. Compared to free Cur (Fig. 1A), the Cur entrapped in Cur/Z and Cur/L nanoparticles was stable against UV irradiation. In addition it was found that Cur in Cur/Z-L composite nanoparticles was more stable than that in Cur/Z and Cur/L nanoparticles during UV irradiation. The retention rate of Cur in the composite nanoparticles was increased with the rise of lecithin level. After 90 min of UV irradiation, more than 57% of Cur was retained in the Cur/Z-$L_{1:2}$ composite nanoparticles as compared to 17% for free Cur, 19% for Cur/Z nanoparticles and 34% for Cur/L nanoparticles. The aromatic side groups and double bonds in zein molecules can absorb UV light, leading to its high stability against UV light (Luo et al., 2013). The presence of lecithin provided a better protection from the degradation of Cur induced by UV irradiation. These findings were consistent with the reports by Xiao et al. (2015) and Patel, Hu et al. (2010) and Patel, Bouwens et al. (2010).

Table 1
Particle size, turbidity, ζ-potential, encapsulation efficiency (EE) and loading efficiency (LE) of curcumin loaded zein-lecithin (Cur/Z-L) composite nanoparticles.

Samples	Particle size (nm)	Turbidity (NTU)	ζ-Potential (mV)	EE (%)	LE (%)
Cur/Z	177.90 ± 2.55^{a}	464.00 ± 8.72^{a}	26.53 ± 1.06^{a}	42.03 ± 1.8^{a}	4.20 ± 0.18^{a}
Cur/$Z_{10:1}$	227.77 ± 2.65^{b}	928.33 ± 16.07^{b}	23.30 ± 0.46^{b}	46.64 ± 2.70^{a}	4.24 ± 0.36^{a}
Cur/$Z_{5:1}$	424.27 ± 5.44^{c}	974.33 ± 7.64^{c}	16.30 ± 1.59^{c}	94.24 ± 2.70^{b}	7.65 ± 0.27^{b}
Cur/$Z_{2:1}$	288.80 ± 3.22^{d}	681.67 ± 3.79^{d}	7.52 ± 0.22^{d}	97.03 ± 1.20^{bc}	6.94 ± 0.26^{c}
Cur/$Z_{1:1}$	141.57 ± 0.46^{e}	389.00 ± 8.54^{e}	5.11 ± 0.14^{e}	99.80 ± 1.1^{c}	4.99 ± 0.18^{d}
Cur/$Z_{2:3}$	124.30 ± 0.51^{f}	255.33 ± 3.06^{f}	5.34 ± 0.87^{e}	99.22 ± 1.2^{c}	4.33 ± 0.10^{a}
Cur/$Z_{1:2}$	130.10 ± 0.95 g	293.67 ± 5.03 g	5.75 ± 0.81^{f}	99.83 ± 1.7^{c}	3.59 ± 0.12^{e}
Cur/L	237.47 ± 3.22 h	298.33 ± 6.81 g	−2.19 ± 0.13 g	86.78 ± 2.6^{d}	8.68 ± 0.28^{f}

Values with different letters in the same column are significantly different ($P < 0.05$).

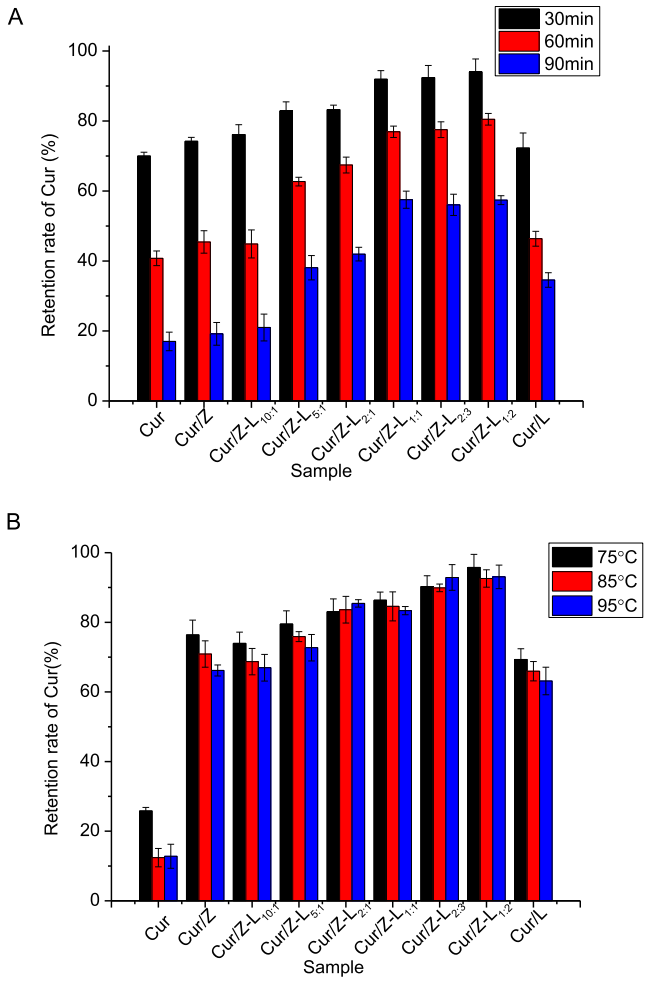

Fig. 1. Retention rate of curcumin in samples of pure curcumin (Cur), Cur loaded in zein (Cur/Z), lecithin (Cur/L) and zein-lecithin (Cur/Z-L) nanoparticles during UV irradiation (A) and thermal treatment (B).

Colloidal delivery systems may experience thermal treatment during food and beverage processing. Therefore, the effect of different temperatures (75, 85 and 95 °C) on the stability of Cur in the nanoparticles was also investigated (Fig. 1B). After the thermal treatment at 75, 85 and 95 °C for 30 min, the retention rates of Cur in free Cur were 25.82, 12.40 and 12.08%, respectively (Fig. 1B). When Cur was loaded in zein nanoparticles, the retention rate of Cur was significantly ($P < 0.05$) increased. The retention rate of Cur in Cur/Z and Cur/L nanoparticles after treating at 95 °C for 30 min was 66.17% and 63.15%, respectively. Furthermore, the protective effect of the Cur/Z-L composite nanoparticles was more significant than that of Cur/Z and Cur/L nanoparticles. At the mass ratio of zein to lecithin of 1:1, the retention rate of Cur could reach to 86.35, 84.58 and 83.35%, respectively, when incubated at 75, 85 and 95 °C for 30 min. This result confirmed that the presence of lecithin made the composite nanoparticles more compact and provided a better protection of Cur during thermal treatment. Furthermore, the resultant Cur/Z-L composite nanoparticles (Cur/Z-$L_{1:1}$, Cur/Z-$L_{2:3}$ and Cur/Z-$L_{1:2}$) have smaller sizes, resulting in smaller surface areas and therefore reduced the contact of environmental stresses.

3.4. Fluorescence spectrum, XRD, FTIR and DSC

Fluorescence spectroscopy analysis was used to confirm the encapsulation and binding of Cur with zein and lecithin in nanoparticle formulations. The fluorescence emission spectra of pure Cur, Cur/Z and Cur/Z-L nanoparticle dispersions were presented in Fig. 2A. The spectrum of pure Cur showed the maximum peak at 550.6 nm at an excitation wavelength of 420 nm. There was a blue shift of the Cur emission maximum peak (520.2 nm) and a significantly ($P < 0.05$) increase in the fluorescence intensity when Cur was encapsulated in zein nanoparticles. Xiao et al. (2015) also reported that the fluorescence spectrum of pure Cur in the solution showed the maximum peak at 555 nm and a blue shift of the emission maximum peak was observed in kafirin/Cur nanoparticles, which indicated that the structure of Cur was changed. In the presence of lecithin, the maximum emission peak of Cur/Z-L composite nanoparticles varied with the mass ratio of zein to lecithin. Compared with pure Cur, the maximum peak of Cur/Z-L composite nanoparticles was significantly ($P < 0.05$) blueshifted from 550.6 to 528.6, 523.2, 520.0, 515.4, and 511.8 nm, for samples of zein to lecithin ratios at 5:1, 2:1, 1:1, 2:3, and 1:2, respectively. The remarkable blueshift, an indicator of the complex formation, might be due to the interactions (e.g., hydrogen bonding, hydrophobic effects, and electrostatic interactions) among zein, lecithin and Cur during the encapsulation and binding of Cur with zein and lecithin (Xiao et al., 2015).

The XRD patterns of samples were shown in Fig. 2B. The major characteristic peaks of Cur occurred at 8.90, 12.26, 14.54, 17.24, 23.33, 24.60 and 25.52°, which indicated its highly crystalline nature (Patel, Hu et al., 2010 and Patel, Bouwens et al., 2010). The XRD patterns of zein exhibited two wider humps at diffraction angles (2θ) of 9.2° and 19.5°, rather than sharp peaks, suggesting the amorphous nature of the protein (Luo et al., 2013). Lecithin was also in an amorphous state because of the lacking of crystalline peaks (Wang, Luo, & Xiao, 2014). From Fig. 2B, it can be found that the XRD diffractograms of Cur/Z and Cur/Z-L nanoparticles did not show tiny characteristic crystalline peaks of Cur, testifying the formation of the amorphous Cur during the encapsulation process. This phenomenon might be ascribed to intermolecular interactions among Cur, zein and lecithin within the particle matrix. Similar results were also observed by Liang, Zhou, He et al. (2015) and Patel, Hu et al. (2010) and Patel, Bouwens et al. (2010), who reported that the crystalline Cur was converted to amorphous state after being entrapped in a nanoscale polymeric matrix, due to the suppression of its crystallisation in the nanoconfinement. In addition, no peak at the diffraction angle of 9.1° was observed for zein-lecithin nanoparticles, which occurred in the diffractogram of individual zein, indicating interactions between zein and lecithin.

The intermolecular interactions among zein, lecithin and Cur were also characterized by FTIR. As illustrated in Fig. 2C, the FTIR spectrum of zein showed a prominent absorption peak at 3326 cm^{-1}, which corresponded to the -OH group (Luo et al., 2011). In the presence of both lecithin and Cur, the peak of hydrogen bonds was significantly shifted to 3314, 3313, 3312 cm^{-1}, respectively, implying that strong hydrogen bonding was generated among zein, lecithin and Cur. Typical absorption peaks (amide I and amide II) of zein occurred at 1658 and 1532 cm^{-1}. The amide I band was associated with the C═O stretching and amide II absorption peak was due to the bond C—N—H in-plane bending, C—N and C—C stretching (Yin, Lu, Liu, & Lu, 2015). Compared with the spectrum of zein, the spectrum of Cur/Z nanoparticles showed that the bands of amide I and amide II groups were shifted from 1658 and 1532 cm^{-1} to 1645 and 1515 cm^{-1}, respectively, suggesting that the electrostatic interaction between zein and Cur. Moreover, zein and Cur were both hydrophobic components and there could exist hydrophobic interactions between zein and Cur. The bands of amide I and amide II groups were shifted from 1658 and 1532 cm^{-1} to 1658 and 1541 cm^{-1}, respectively, in Cur/Z-L composite nanoparticles, indicating the electrostatic interaction occurred among zein, lecithin and Cur. Liang, Zhou, Li et al. (2015) reported that the amide

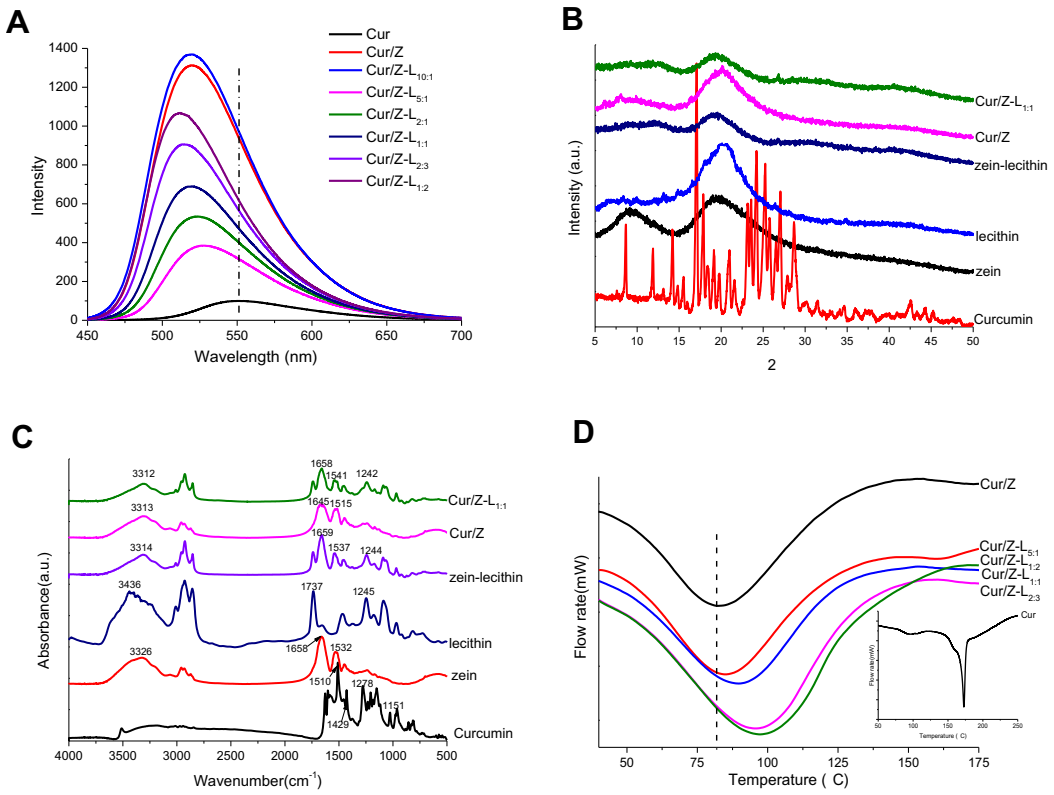

Fig. 2. Florescence spectra (A), XRD (B), FTIR (C) and DSC (D) spectra of samples.

I and amide II bands of zein in Cur/Z nanoparticles were significantly ($P < 0.05$) shifted from 1646 and 1559 cm^{-1} to 1639 and 1541 cm^{-1}, respectively. This result confirmed that the electrostatic interaction was involved in the intermolecular forces between Cur and zein. Moreover, for both Cur/Z and Cur/Z-L nanoparticles, amide I and amide II bonds presented a much wider peak and the absorption intensity of amide I and amide II decreased, in comparison to the spectrum of native zein. These results were attributed to the formation of hydrogen bonding between phenolic hydroxyl groups in Cur and the carbonyl group in amide bonds of Cur/Z and Cur/Z-L nanoparticles. Myshakina, Ahmed, and Asher (2008) also reported that hydrogen bonding in the carbonyl groups might lead to a decrease in C=O double bond.

The strong peaks at 1737 and 1245 cm^{-1} in the spectrum of lecithin were due to C=O and P=O stretching vibrations. The FTIR spectrum of Cur showed a sharp peak at 3511 cm^{-1}, which was due to O—H stretching (Xiao et al., 2015). Absorption peaks at around 1627 and 1278 cm^{-1} were contributed by ν(C=C) and ν (C—O). The most prominent band in the spectrum of Cur was at 1510 cm^{-1}, which was the result of highly mixed vibrations (Kolev, Velcheva, Stamboliyska, & Spiteller, 2005). The peaks at 1429 and 1151 cm^{-1} were related to the vibrations of δ (C—C—C) and δ(C—O—C) of aromatic rings and the inter-ring chain of pure Cur (Hu et al., 2015). Most characteristic peaks (1510, 1429, 1278 and 1151 cm^{-1}) of Cur disappeared in the spectrum of both Cur/Z and Cur/Z-L. This phenomenon revealed that Cur might be interacted with zein and lecithin by hydrogen bonding or hydrophobic effects. Hu et al. (2015) suggested that the characteristic peaks of Cur at 1427, 1154, 1232, and 856 cm^{-1} disappeared in the spectrum of Cur-fortified nanoparticles due to the hydrogen bonding and hydrophobic interactions among Cur, zein and pectin.

The change in the physical state of bioactive compounds in the formulation can be determined by DSC (Fig. 2D). The DSC curve of Cur showed a sharp endothermic peak at around 172.78 °C (the insert figure in Fig. 2D), which was attributed to the melting of Cur crystals and indicated the presence of Cur in crystalline state (Hu et al., 2015; Xiao et al., 2015). According to Fig. 2D, the characteristic endothermal peak of Cur was not observed in both Cur/Z and Cur/Z-L nanoparticles, which implied that Cur in amorphous form was well dispersed in the nanoparticles. These results were also confirmed by XRD analysis (Fig. 2B), which indicated that Cur formed an amorphous complex with zein and lecithin. The Cur/Z nanoparticles exhibited an endothermal peak at about 82.19 °C. The denaturation temperature of Cur/Z-L composite nanoparticles was increased with the rise of lecithin level, from 82.19 to 85.08, 89.77, 95.73, 97.24 °C, respectively, for the samples of Cur/Z-$L_{5:1}$, Cur/Z-$L_{1:1}$ Cur/Z-$L_{2:3}$ and Cur/Z-$L_{1:2}$, compared with that of Cur/Z nanoparticle. The presence of lecithin could enhance

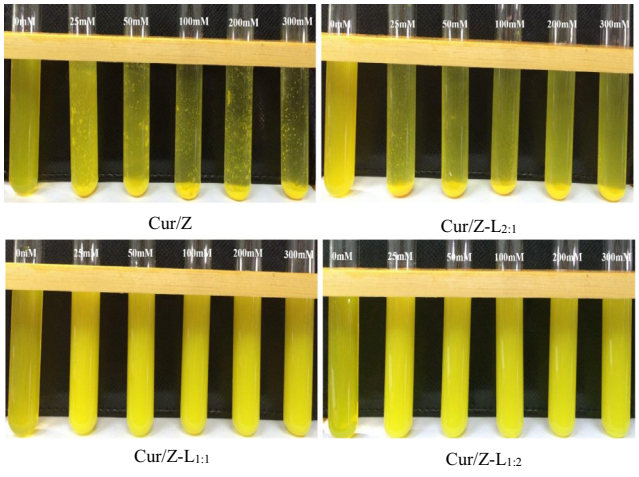

Fig. 3. Effect of NaCl concentration on the stability of curcumin loaded zein (Cur/Z) and zein-lecithin (Cur/Z-L) nanoparticle dispersions.

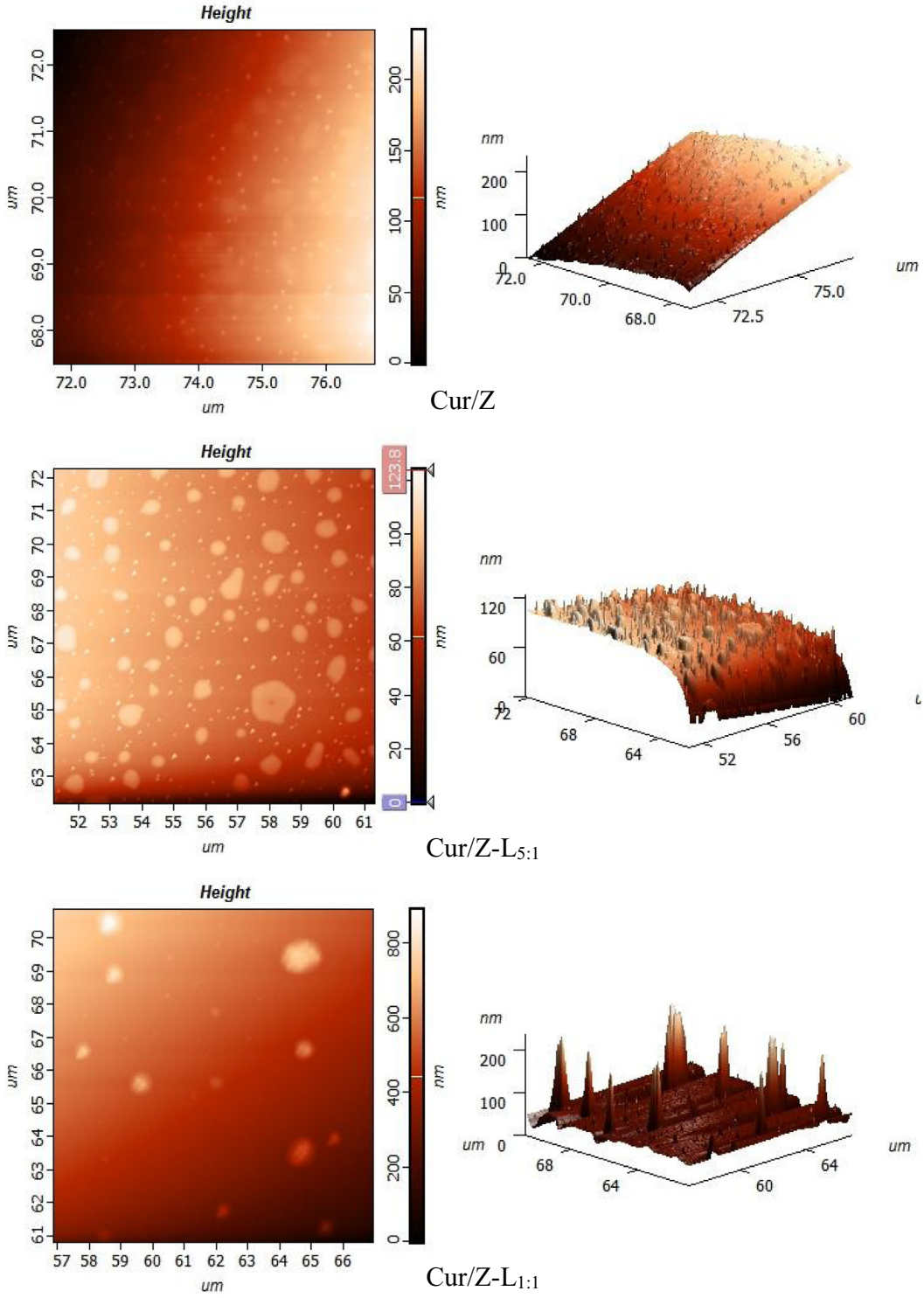

Fig. 4. AFM images of curcumin loaded zein (Cur/Z) and zein-lecithin (Cur/Z-L) nanoparticles.

the interactions such as hydrophobic effects and electrostatic interaction among different components in the nanoparticles, leading to the high endothermic peak temperature. Zhang, An, Cui, and Li (2003) also reported that hydrophobic interaction between β-lactoglobulin and phospholipids increased the thermal stability of the protein.

3.5. Effect of salt on the stability of nanoparticle dispersions

Colloidal delivery systems may encounter various electrolytes in commercial products and human gastrointestinal tract. Therefore, it is important to determine the influence of ionic strength on the physical properties and stability of delivery systems. The influence of salt (NaCl) concentration on the properties of Cur/Z

and Cur/Z-L nanoparticle dispersions was thereby investigated (Fig. 3). Cur-loaded zein nanoparticle dispersions were unstable and formed a yellow sediment at the bottom of the test tube even at relatively low salt concentration (25 mM). With further increase in the salt concentration, the sediment layer became thicker and the supernatant became clearer. After the addition of NaCl, the Cur/Z-$L_{2:1}$ composite nanoparticle dispersions also showed destabilization, forming yellow sediment at the bottom of the test tubes and clearer supernatant. These results might be ascribed to the fact that the ionic strength influenced the interaction among the composite nanoparticles (Chen et al., 2014). In the absence of salt, the electrostatic repulsion among nanoparticles played an important role in stabilizing the nanoparticles against the aggregation. In the presence of salt, the electrostatic interactions among the nanoparticles were screened and the attractive interactions such as van der Waals, hydrophobic effects became strong enough to overcome electrostatic interactions. Therefore it resulted in the extensive nanoparticle aggregation (Chen et al., 2014; Hu & McClements, 2014, 2015). However, continuing to increase the level of lecithin, precipitates were scarcely observed for Cur/Z-$L_{1:1}$, Cur/Z-$L_{2:3}$ and Cur/Z-$L_{1:2}$ composite nanoparticle dispersions at NaCl concentrations from 25 to 300 mM. Excessive lecithin prompted the structure of composite nanoparticles to become more compact, reduced the effect of salt on the interactions among nanoparticles and prevented the aggregation of nanoparticles. Hu and McClements (2015) also reported that the presence of Tween 80 increased the stability of zein nanoparticles.

3.6. Morphological observation

The morphology of Cur/Z, Cur/Z-$L_{5:1}$ and Cur/Z-$L_{1:1}$ nanoparticles was observed by AFM (Fig. 4). The Cur/Z nanoparticles showed a spherical shape with a uniform size. Similar result was also reported by previous researchers (Wang et al., 2014). After the addition of lecithin, the morphology of Cur/Z-L composite nanoparticles was modified. The sample of Cur/Z-$L_{5:1}$ showed irregular geometry shapes and a larger size. When the mass ratio of zein to lecithin was 1:1, the samples exhibited spherical shape with smaller size. This result was consistent with that of particle size measurement by Zetasizer in Table 1.

The morphological structure presented by SEM in Fig. S1 also confirmed the result of AFM. The presence of lecithin resulted in the emergence phenomena and irregular geometry shapes of composite nanoparticles. The nanoparticles were clumped and connected to each other, individual ones could be scarcely observed. The structure of nanoparticles was similar to that reported complex by other studies of zein and oil based substance micro/-nanoparticles as the lecithin was consist of a glycerol backbone esterified with two fatty acids (Luo et al., 2011). The elementary compositions of single nanoparticle of samples were determined using SEM-EDS and the results were shown in Table S1. As we know, lecithin contains element phosphorus. It's expected that Cur/Z nanoparticles exhibited no phosphorus content (%), and the phosphorus was observed in Cur/Z-L composite nanoparticles. And the content of phosphorus in Cur/Z-$L_{1:1}$ composite nanoparticles was higher than that in Cur/Z-$L_{5:1}$. These results could further confirm the formation of pure composite nanoparticles.

3.7. Hypothesis of the formation mechanism of composite nanoparticles

Herein, a schematic diagram for the formation mechanism of Cur/Z and Cur/Z-L composite nanoparticles was proposed to elucidate the possible formation mechanism of composite nanoparticles (Fig. 5). When zein and Cur in aqueous ethanol solutions were dropped into deionized water, zein could self-assemble into colloidal particles. The Cur was encapsulated in the zein colloidal nanoparticles and the Cur/Z nanoparticle exhibited relatively uniform spherical shape. However, based on the results of dynamic light scattering, zeta-potential and turbidity measurement, as well as the morphological observation by AFM, there were two mechanisms proposed for the formation of Cur/Z-L composite nanoparticles due to the different level of lecithin. At a relatively low level of lecithin (zein to lecithin mass ratio $\leq$ 5:1), the alkyl chain of lecithin might be embedded into the hydrophobic region of zein, reducing partially unfolded hydrophobic microdomains and leading the aggregation of composite nanoparticles. Continuing to increase the level of lecithin, the formation mechanism of Cur/Z-L composite nanoparticles was different from that at a low level of lecithin. The interaction among zein, lecithin and Cur

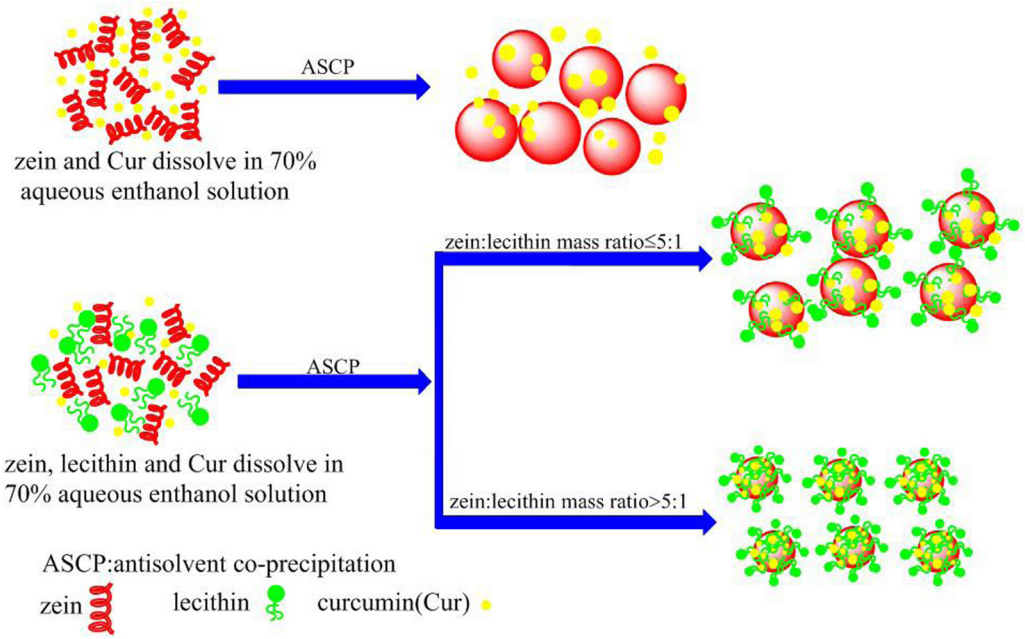

Fig. 5. An illustration of the formation mechanism and possible structures of curcumin loaded zein-lecithin composite nanoparticles.

was increased with the level of lecithin increasing. The alkyl chain of lecithin was interacted with zein and Cur mainly through hydrophobic effects, hydrogen bonding and electrostatic interaction, and formed a more compact structure, exhibiting a smaller size and lower turbidity value, also increasing the LE and EE of Cur and inhibiting nanoparticles aggregation.

4. Conclusion

In the present study, antisolvent co-precipitation was utilized to fabricate Cur/Z-L composite nanoparticles for the delivery of Cur. The inclusion of lecithin in Cur/Z-L composite nanoparticle led to different sizes, turbidity and zeta potential values compared to those of Cur/Z and Cur/L nanoparticles. Moreover, the presence of lecithin significantly enhanced the encapsulation efficiency of Cur. The entrapped Cur was in an amorphous state in the nanoparticles and interacted with zein and lecithin mainly through hydrogen bonding, electrostatic interaction and hydrophobic effects for the formation of Cur/Z-L composite nanoparticles. Cur in the Cur/Z-L composite nanoparticles also exhibited better UV-light and thermal stability as compared to pure Cur and Cur in Cur/Z nanoparticles. These findings can broaden the application of zein and the composite nanoparticles are potential for delivering bioactive compounds in functional food and beverage products.

Acknowledgements

The research was funded by the National Natural Science Foundation of China (No. 31371835).

Appendix A. Supplementary data

Supplementary data associated with this article can be found, in the online version, at http://dx.doi.org/10.1016/j.foodchem.2017.05.134.

References

Aditya, N. P., Shim, M., Lee, I., Lee, Y., Im, M. H., & Ko, S. (2013). Curcumin and genistein coloaded nanostructured lipid carriers: In vitro digestion and antiprostate cancer activity. *Journal of Agricultural and Food Chemistry, 61*(8), 1878–1883.

Anand, P., Kunnumakkara, A. B., Newman, R. A., & Aggarwal, B. B. (2007). Bioavailability of curcumin: Problems and promises. *Molecular Pharmaceutics, 4*(6), 807–818.

Chen, X., Zou, L.-Q., Niu, J., Liu, W., Peng, S.-F., & Liu, C.-M. (2015). The stability, sustained release and cellular antioxidant activity of curcumin nanoliposomes. *Molecules, 20*(8), 14293–14311.

Chen, J., Zheng, J., McClements, D. J., & Xiao, H. (2014). Tangeretin-loaded protein nanoparticles fabricated from zein/β-lactoglobulin: Preparation, characterization, and functional performance. *Food Chemistry, 158*, 466–472.

Chen, H., & Zhong, Q. (2014). Processes improving the dispersibility of spray-dried zein nanoparticles using sodium caseinate. *Food Hydrocolloids, 35*, 358–366.

Cheng, A. L., Hsu, C. H., Lin, J. K., Hsu, M. M., Ho, Y. F., Shen, T. S., et al. (2001). Phase I clinical trial of curcumin, a chemopreventive agent, in patients with high-risk or pre-malignant lesions. *Anticancer Research, 21*(4B), 2895–2900.

Dai, L., Sun, C., Wang, D., & Gao, Y. (2016). The Interaction between zein and lecithin in ethanol-water solution and characterization of zein-lecithin composite colloidal nanoparticles. *PLoS ONE, 11*(11), e0167172.

Gao, Z. M., Yang, X. Q., Wu, N. N., Wang, L. J., Wang, J. M., Guo, J., & Yin, S. W. (2014). Protein-based pickering emulsion and oil gel prepared by complexes of zein colloidal particles and stearate. *Journal of Agricultural and Food Chemistry, 62*(12), 2672–2678.

Gomez-Estaca, J., Balaguer, M. P., Gavara, R., & Hernandez-Munoz, P. (2012). Formation of zein nanoparticles by electrohydrodynamic atomization: Effect of the main processing variables and suitability for encapsulating the food coloring and active ingredient curcumin. *Food Hydrocolloids, 28*, 82–91.

Hu, K., & McClements, D. J. (2014). Fabrication of surfactant-stabilized zein nanoparticles: A pH modulated antisolvent precipitation method. *Food Research International, 64*, 329–335.

Hu, K., & McClements, D. J. (2015). Fabrication of biopolymer nanoparticles by antisolvent precipitation and electrostatic deposition: Zein-alginate core/shell nanoparticles. *Food Hydrocolloids, 44*, 101–108.

Hu, K., Huang, X., Gao, Y., Huang, X., Xiao, H., & McClements, D. J. (2015). Core–shell biopolymer nanoparticle delivery systems: Synthesis and characterization of curcumin fortified zein–pectin nanoparticles. *Food Chemistry, 182*, 275–281.

Hu, D., Lin, C., Liu, L., Li, S., & Zhao, Y. (2012). Preparation, characterization, and in vitro release investigation of lutein/zein nanoparticles via solution enhanced dispersion by supercritical fluids. *Journal of Food Engineering, 109*(3), 545–552.

Jafari, Y., Sabahi, H., & Rahaie, M. (2016). Stability and loading properties of curcumin encapsulated in Chlorella vulgaris. *Food Chemistry, 211*, 700–706.

Kolev, T. M., Velcheva, E. A., Stamboliyska, B. A., & Spiteller, M. (2005). DFT and experimental studies of the structure and vibrational spectra of curcumin. *International Journal of Quantum Chemistry, 102*(6), 1069–1079.

Li, J., Hwang, I. C., Chen, X., & Park, H. J. (2016). Effects of chitosan coating on curcumin loaded nano-emulsion: Study on stability and in vitro digestibility. *Food Hydrocolloids, 60*, 138–147.

Liang, H., Zhou, B., He, L., An, Y., Lin, L., Li, Y., & Li, B. (2015). Fabrication of zein/quaternized chitosan nanoparticles for the encapsulation and protection of curcumin. *RSC Advances, 5*(18), 13891–13900.

Liang, H., Zhou, B., Li, J., Xu, W., Liu, S., Li, Y., & Li, B. (2015). Supramolecular design of coordination bonding architecture on zein nanoparticles for pH-responsive anticancer drug delivery. *Colloids and Surfaces B: Biointerfaces, 136*, 1224–1233.

Luo, Y., Wang, T. T., Teng, Z., Chen, P., Sun, J., & Wang, Q. (2013). Encapsulation of indole-3-carbinol and 3, 3′-diindolylmethane in zein/carboxymethyl chitosan nanoparticles with controlled release property and improved stability. *Food Chemistry, 139*(1), 224–230.

Luo, Y., Zhang, B., Whent, M., Yu, L. L., & Wang, Q. (2011). Preparation and characterization of zein/chitosan complex for encapsulation of alpha-tocopherol, and its in vitro controlled release study. *Colloids and Surfaces B, 85*(2), 145–152.

Patel, A., Hu, Y., Tiwari, J. K., & Velikov, K. P. (2010). Synthesis and characterisation of zein–curcumin colloidal particles. *Soft Matter, 6*(24), 6192–6199.

Patel, A. R., Bouwens, E. C., & Velikov, K. P. (2010). Sodium caseinate stabilized zein colloidal particles. *Journal of Agricultural and Food Chemistry, 58*(23), 12497–12503.

Podaralla, S., & Perumal, O. (2012). Influence of formulation factors on the preparation of zein nanoparticles. *Aaps Pharmscitech, 13*(3), 919–927.

Myshakina, N. S., Ahmed, Z., & Asher, S. A. (2008). Dependence of amide vibrations on hydrogen bonding. *Journal of Physical Chemistry B, 112*, 11873–11877.

Sadeghi, R., Moosavi-Movahedi, A. A., Emam-Jomeh, Z., Kalbasi, A., Razavi, S. H., Karimi, M., & Kokini, J. (2014). The effect of different desolvating agents on BSA nanoparticle properties and encapsulation of curcumin. *Journal of Nanoparticle Research, 16*(9), 1–14.

Sebaaly, C., Jraij, A., Fessi, H., Charcosset, C., & Greige-Gerges, H. (2015). Preparation and characterization of clove essential oil-loaded liposomes. *Food Chemistry, 178*, 52–62.

Shahgholian, N., & Rajabzadeh, G. (2016). Fabrication and characterization of curcumin-loaded albumin/gum arabic coacervate. *Food Hydrocolloids, 59*, 17–25.

Sun, C., Dai, L., & Gao, Y. (2016). Binary complex based on zein and propylene glycol alginate for delivery of quercetagetin. *Biomacromolecules, 17*(12), 3973–3985.

Sun, C., Liu, F., Yang, J., Yang, W., Yuan, F., & Gao, Y. (2015). Physical, structural, thermal and morphological characteristics of zeinquercetagetin composite colloidal nanoparticles. *Industrial Crops and Products, 77*, 476–483.

Souza, M. P., Vaz, A. F., Correia, M. T., Cerqueira, M. A., Vicente, A. A., & Carneiro-da-Cunha, M. G. (2014). Quercetin-loaded lecithin/chitosan nanoparticles for functional food applications. *Food Bioprocess Technology, 7*(4), 1149–1159.

Wang, W., Liu, F., & Gao, Y. (2016). Quercetagetin loaded in soy protein isolate–κ-carrageenan complex: Fabrication mechanism and protective effect. *Food Research International, 83*, 31–40.

Wang, X., Luo, Z., & Xiao, Z. (2014). Preparation, characterization, and thermal stability of β-cyclodextrin/soybean lecithin inclusion complex. *Carbohydrate Polymers, 101*, 1027–1032.

Wilken, R., Veena, M. S., Wang, M. B., & Srivatsan, E. S. (2011). Curcumin: a review of anti-cancer properties and therapeutic activity in head and neck squamous cell carcinoma. *Molecular Cancer, 10*(12), 1–19.

Xiao, J., Nian, S., & Huang, Q. (2015). Assembly of kafirin/carboxymethyl chitosan nanoparticles to enhance the cellular uptake of curcumin. *Food Hydrocolloids, 51*, 166–175.

Xue, J., & Zhong, Q. (2014). Blending lecithin and gelatin improves the formation of thymol nanodispersions. *Journal of Agricultural and Food Chemistry, 62*(13), 2956–2962.

Yin, H., Lu, T., Liu, L., & Lu, C. (2015). Preparation, characterization and application of a novel biodegradable macromolecule: Carboxymethyl zein. *International Journal of Biological Macromolecules, 72*, 480–486.

Zhang, Y., An, Z., Cui, G., & Li, J. (2003). Stabilized complex film formed by coadsorption of β-lactoglobulin and phospholipids at liquid/liquid interface. *Colloids and Surfaces A, 223*, 11–16.

Zhang, Z., Zhang, R., Zou, L., Chen, L., Ahmed, Y., Al Bishri, W., & McClements, D. J. (2016). Encapsulation of curcumin in polysaccharide-based hydrogel beads: Impact of bead type on lipid digestion and curcumin bioaccessibility. *Food Hydrocolloids, 58*, 160–170. Ellipsis.

Zou, L., Zhang, Z., Zhang, R., Liu, W., Liu, C., Xiao, H., & McClements, D. J. (2016). Encapsulation of protein nanoparticles within alginate microparticles: Impact of pH and ionic strength on functional performance. *Journal of Food Engineering, 178*, 81–89.